MRS Advances © The Author(s), 2020, published on behalf of Materials Research Society by Cambridge University Press
DOI: 10.1557/adv.2020.413

Synthesis and characterization of $La_{0.7}Sr_{0.3}Fe_{0.7}Co_{0.3}O_{3\pm\delta}$ by Sonochemistry

De La Huerta Hernández G. Elena[1]*, Castro Cisneros Iván[2], Chávez Carvayar José A.[3], Hernández Pérez Isaías[1]

[1]*Departamento de Ciencias Básicas, UAM-A, Av. San Pablo No. 180, Azcapotzalco, Ciudad de México. C.P. 02200. México.*
[2]*Facultad de Ingeniería, Universidad Autónoma del Carmen, , Av. Central s/n esq. Con Fracc. Mundo Maya, Ciudad del Carmen. C.P. 24115. México*
[3]*Instituto de Investigaciones en Materiales, UNAM, Circuito exterior, C.U., Ciudad de México. C.P. 04510. México.*

** Author for correspondence: gloriaelenadelahuerta@gmail.com*

Abstract

Among different possible energy sources, in the search for fossil fuel substitutes, hydrogen and fuel cells are presented as one of the most promising alternatives, with great potential, in the development of devices for the generation of clean electrical energy. Recently, lanthanum based compounds have been studied due to their interesting transport properties, which led these products to be applied as possible cathode materials in a solid oxide fuel cell. In this work, a lanthanum based material with a perovskite structure, $La_{0.7}Sr_{0.3}Fe_{0.7}Co_{0.3}O_{3\pm\delta}$ (LSFC), was synthesized, from nitrates, by sonochemistry. This product was structurally characterized by powder X-ray diffraction and morphological studies were obtained by scanning electron microscopy. Results showed a nanostructured material with a crystal size in de order of 14 nm and a cubic perovskite structure with cell parameters of a = 3.8927 Å. Morphological characterization indicated a porous material formed by grains of homogeneous size, pores had an average length of 17 nm and area of 36 nm2, showing a channel shape distribution.

INTRODUCTION

Growing concern about the need for a cleaner environment and clean energy is driving to, develop new and ecofriendly energy conversion devices. Fuel cells are devices, which converting chemical energy into electrical energy and heat, without requiring the combustion of fossil fuels. Solid oxide fuel cells (SOFCs) based on oxide electrolytes, attracted considerable attention due to their higher efficiency and arise as alternative to reduce high levels of greenhouse gases. Due to have several advantages over other types of fuel cells, such as relatively inexpensive materials, low sensitivity to impurities in the fuel, and high efficiency [1–3], low environmental impact and are expected to become the emerging technology for stationary power production [4]. Fuel cells, as generators of electrical energy, can operate in semi-isolated or completely isolated towns; in this way, it is possible to supply electrical energy to rural communities, which may have a better quality of life. Also, these energy sources can solve problems in these remote places since they can provide not only electrical energy required by a hospitals, specialized clinics, but also increase telecommunication channels [5-7].

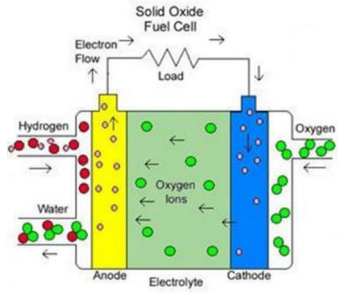

Figure 1. Conformation basic of a SOFC[8]

The role of the cathode as the active site for the electrochemical reduction of oxygen is an important parameter to take into account during the material´s design. SOFCs must be operate at high temperatures for long periods of time and, therefore, some requirements must be fulfilled [9], as well as: high electronic conductivity (σ > 100 S cm-1), a thermal expansion coefficient (TEC) match with other SOFC components, chemical compatibility with the electrolyte and interconnect materials, adequate porosity to allow mass transport of oxygen, high thermal stability, high catalytic activity for the oxygen reduction reaction (ORR) and low cost. Several materials have been selected as promising candidates as cathodes in order to limit the overpotential a yttria-stabilized zirconia (YSZ) electrolyte has been used with a Lanthanum manganite (LSM) cathode operating at 800-1000 °C, which have a suitable porous structure, good electrical conductivity and competitive costs [9]. The *p*-type conductivity of $LaMnO_3$ is related, to cation vacancies; therefore, if doped with cations with lower charge than La^{3+} in A or B sites, the conductivity will increase. Group 2 earth-alkaline ions (Mg, Ca, Sr and Ba) are widely used for A-site doping. These cations with 2+ valence occupy La^{3+} positions in the net, thus provoking oxidation of some Mn^{3+} to Mn^{4+} to maintain charge balance. Electrical conductivity of these manganites is due to the hopping of one electron between the 3+ and 4+ state of manganese.The main weakness of SOFC is the high operating temperatures, which leads to material degradation (electrode sintering), insulating phase formation at the

electrode-electrolyte interface, interdiffusion effects, secondary phases and other drawback [10]. In order to operate efficiently at lower temperatures and to develop the next generation of SOFC´s energy devices, new materials are required and the utilized processing routes must be optimized [4,11]. Manganites, lanthanum cobaltites doped with bivalent metals such as Ca or Sr emerged [12]. These materials exhibit high conductivity values when 30% or 40% of Ca or Sr are added respectively. In addition, the substitution of La by other lanthanides such as Pr and Sm has also lead to promising results. Despite the good results that these cobaltites exhibit, other drawbacks such as their high TECs and the appearance of secondary phases, limit their application. In order to avoid these disagreements, new materials and new synthesis procedures for low operational temperatures are in development. The present research explores the possibility of using $La_{0.7}Sr_{0.3}Fe_{0.7}Co_{0.3}O_{3\pm\delta}$ as low-cost alternative cathode for intermediate temperature SOFCs. The main goal is to bring these new "potential electrode" materials into a functional fuel cell.

EXPERIMENTAL

Materials and Methods

$La_{0.7}Sr_{0.3}Fe_{0.7}Co_{0.3}O_{3\pm\delta}$ (LSFC) type perovskite material, was synthesized, by sonochemical method, employing lanthanum nitrate ($La(NO_3)_3 \cdot 6H_2O$, 99.99%) Alfa-Aesar Cas.10277-43-7), strontium nitrate ($Sr(NO_3)_2$, 99% Sigma-Aldrich Cas. 243-42-6), iron nitrate ($Fe(NO_3)_2 \cdot 9H_2O$, 98% Sigma-Aldrich Cas. 216-82-8) and cobalt nitrate ($Co(NO_3)_3 \cdot 6H_2O$, ≥98% Sigma-Aldrich Cas.10026-22-9) as precursors. Additionally it was used ethylene glycol (1-2 ethanediol JT Baker Cas.107-21-1) as surfactant, ammonium hydroxide (NH_4OH 28-30% Sigma-Aldrich Cas.1336-21-6) as precipitating agent; a methanol/acetone mixture (50/50 v/v) was used as dissolvent. All chemicals were employed as supplied without further purification.

Sonochemical synthesis

Among the traditional synthesis methods are solid state, hydrothermal synthesis, combustion, sol-gel, among others. However, in recent dates, different materials have been obtained through sonochemistry, which is a novel method that assists and promuve chemical reactions by ultrasonic cavitation and their effects directly influence the morphology of the particles during growth phase. Among the advantages of using sonosynthesis are: greater control of the crystal structure, the acceleration of chemical reactions, improvement in mass transfer, decrease in reaction cycles [13,14].

For this synthesis is necessary considered the molar relationship between products and reactants. In this case, the equation for obtained the phase $La_{0.7}Sr_{0.3}Fe_{0.7}Co_{0.3}O_{3\pm\delta}$ (LSFC) is:

$$La(NO_3)_3 + Sr(NO_3)_2 + Fe(NO_3)_3 + Co(NO_3)_2 \rightarrow La_{1-x}Sr_xFe_{1-y}Co_y$$

For the synthesis initially, all nitrates (precursors) were dissolved into, a methanol/acetone solution. After this the, solution was put in an ultrasonic bath (Branson CPXH, 1.8 L, 40 Khz) and ethylene glycol was added, the resulting mixture was sonicated for 50min, then a 1M solution of NH_4OH was added dropwise, until

precipitation, maintaining a constant magnetic stirring. The precipitate was washed (4 times with deionized water). Afterward, filtered and dried at 40°C. Finally, the former was heat treated (calcined) for 3h at 500°C in static air and a heating rate of 5°C/min.

Structural and Morphological analysis

The obtained samples were morphological and structural characterized, by means of powder X-ray diffraction, using a Bruker D8 Advance diffractometer with CuKα radiation (1.5406Å), in Bragg-Brentano geometry (θ-2θ) in the range of 20°-80° and 20°-120° with a 0.02 °step and a time collection step of 1.2s. The results were analyzed using Diffract Plus software and compared to the ICSD database standards, Bragg´s formula (equation 1) was employed to estimate the crystal size and cell parameters.

$$D = \frac{k\lambda}{\beta(cos\theta)} \qquad (1)$$

By means of scanning electron microscopy (SEM), the morphological analysis of synthesized samples was performed, using a JEOL 7600F microscope; micrographs were measured in a field emission mode, with resolution of 2.3 Å, 1,000,000X amplification and 10KV acceleration voltage and secondary electrons detector

RESULTS AND DISCUSSIONS

Structural and morphological characterization

Displays the crystallographic behaviour of $La_{0.7}Sr_{0.3}Fe_{0.7}Co_{0.3}O_{3\pm\delta}$, as can be seen at the bottom of Fig.2, the as prepared sample shows a signal with high noise, which is associated with low crystallinity, which may be due to the presence of ethylene glycol. Therefore, it was necessary to perform a heat treatment, in the range of 500 to 800 °C, with steps of 100 °C each. With this, it was possible to determine the crystallization temperature, as well as the different phase transformations. In this way, the crystal growth was studied, founding that at 500 °C, the phase crystallization begins to be induced (see yellow pattern in Fig. 2).

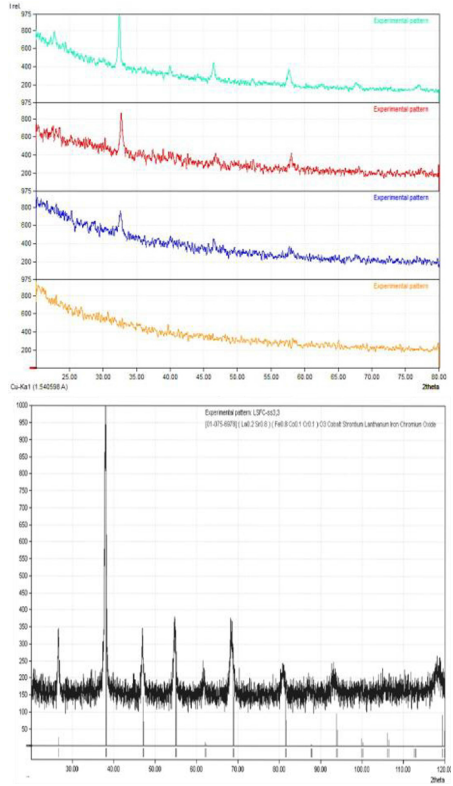

Figure 2. a) Crystal growth profile in $La_{0.7}Sr_{0.3}Fe_{0.7}Co_{0.3}O_{3\pm\delta}$ at 500°C(yellow), 600°C(blue), 700°C (red) and 800°C(green) b) X-ray profile showing phase identification of sample $La_{0.7}Sr_{0.3}Fe_{0.7}Co_{0.3}O_{3\pm\delta}$ heat treated at 800 °C.

On the other hand, structural analysis in Figure 2b shows that at highest temperatures than 500 °C, sample achieves a good crystallization. From the above results, the minimum crystallization and calcination temperature was established in 600 °C.

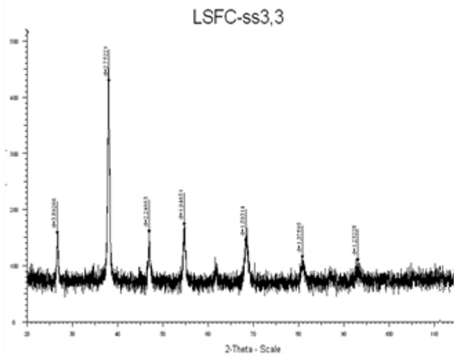

Miller index [h k l]	Interplanar Distance (Å) $La_{0.7}Sr_{0.3}Fe_{0.7}Co_{0.3}O_{3\pm\delta}$
1 0 0	3.89266
1 1 0	2.75221
1 1 1	2.24663
2 0 0	1.94651
2 1 1	1.59314
2 2 0	1.37895
3 1 0	1.23228

Figure 3. Rietveld refinement and assignation of Interplanar distances of cubic phase of $La_{0.7}Sr_{0.3}Fe_{0.7}Co_{0.3}O_{3\pm\delta}$

Additionally, from Fig. 3, all reflections (peaks) located at 38, 47, 55, 62, 68, 82 and 93 °2θ, were identified and indexed to the corresponding crystallographic planes, which are summarized in Table 1 and Figure 3. These planes were assigned to cubic phase of $La_{0.7}Sr_{0.3}Fe_{0.7}Co_{0.3}O_{3\pm\delta}$, which totally match with ICSD 01-089-5720 standard regardless of the heat treatment temperature. Which corresponds to a cubic phase, space group Pm-3m (221), cell parameter a=3.8927Å, cell volume V=58.9865Å^3, and crystallite size of 13 nm, which was calculated from the Debye-Scherrer approximation for cubic symmetries and FWHM=0.64.

Figure 4 show SEM micrographs of the calcined sample at 600 °C, observing at the left side the presence of homogeneous size and fine particles, with a semispherical shape and forming agglomerates with a poor porosity, this can be influenced by the ethylene glycol residual.

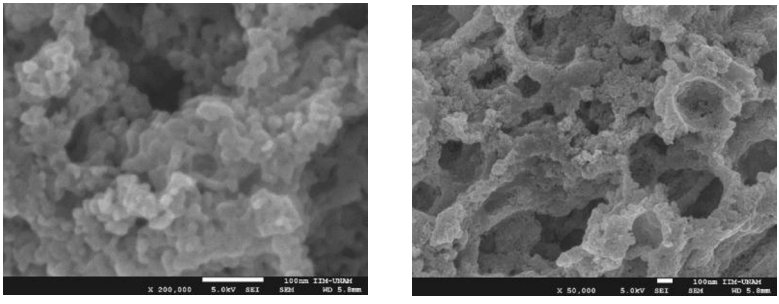

Figure 4.SEM micrographs showing a) the stacked morphology and b) the pore structure of $La_{0.7}Sr_{0.3}Fe_{0.7}Co_{0.3}O_{3\pm\delta}$ heat-treated at 800 °C

On the right side of Figure 4 is showed the micrograph for the sample heat treated at temperature of 800 °C, from this picture is evident the formation of round elongated shape in the grains of cathode material, which can be distinguished by their with irregularly shaped morphology and large porous structure. The latter can be attributed to the total removal of the surfactant (ethylene glycol), leaving these empty spaces in the cathode matrix of $La_{0.7}Sr_{0.3}Fe_{0.7}Co_{0.3}O_{3\pm\delta}$ phase.

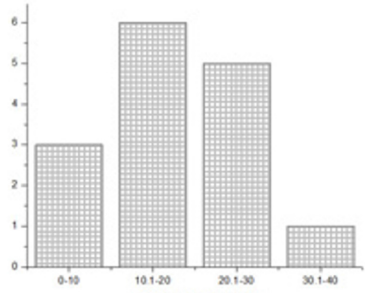

Figure 5. Pore length distribution in nanometers.

From the above micrograph 15 aleatory measurements were taken, with an average pore length of 16.89nm and area of 35.74nm^2, with a pore distribution mostly between 10-20nm in length, in it, the pores have small dimensions because in most are displayed in the form of channels. (see Fig. 5).

Whit the structural and morphological results, it is possible to conclude that increasing the heat treatment temperature, promotes the increase of porosity and the formation of rounded elongated shape structures of $La_{0.7}Sr_{0.3}Fe_{0.7}Co_{0.3}O_{3\pm\delta}$ perovskites, which could be beneficial for free air flow though cathode material. After heat treatment, from X-ray diffraction, no evidence of degradation and secondary phase transformation were observed, neither changes in composition and nor changes in structure have been detected.

CONCLUSIONS

$La_{0.7}Sr_{0.3}Fe_{0.7}Co_{0.3}O_{3\pm\delta}$ single-phase compound was synthesized by sonochemistry. XRD results showed a nanostructured material with a crystal size of 13 nm; also a cubic perovskite structure with cell parameters of a = 3.8927 Å was determined. SEM micrographs showed a porous material formed by grains of homogeneous size, pores had an average length of 17 nm and area of 36 nm^2, showingh irregularly shaped morphology and large porous structure and a channel shape distribution. Due to the presence of ethylene glycol, it is assumed to have a coating character, which prevents crystal growth and, in turn, does not allow thermal analysis, so it is necessary to follow the formation of the crystalline phase through DRX. At this stage, structural and morphological results indicate that this material present appropriate characteristics to be used as cathode material in a SOFC. In addition, impedance spectroscopy studies are in progress, in order to identify its transport properties.

ACKNOWLEDGMENT:

G.H. DE LA Huerta Hernández thanks to CONACYT for the scholarship awarded at UAM-A for PhD studies, we acknowledge to DCBI-UAM-A, IIM-UNAM for the financial support and O. Novelo and A Tejeda for the technical assistance.

References

[1] A. Hagen, H. Langnickel, and X. Sun, "Operation of solid oxide fuel cells with alternative hydrogen carriers," Int. J. Hydrogen Energy, vol. 44, no. 33, pp. 18382–18392, 2019, doi: 10.1016/j.ijhydene.2019.05.065.

[2] R. Fernández-González, T. Molina, S. Savvin, R. Moreno, A. Makradi, and P. Núñez, "Characterization and fabrication of LSCF tapes," J. Eur. Ceram. Soc., vol. 34, no. 4, pp. 953–959, 2014, doi: 10.1016/j.jeurceramsoc.2013.10.023

[3] Mogensen M, Kammer K (2003), Conversion of Hydrocarbons in Solid Oxide Fuel Cells Annu Rev Mater Res 33:321

[4] Ortiz-Vitoriano N, Bernuy-López C, Ruiz de Larramendi I, Knibbe R, Thydén K, Hauch A, Holtappels P, Rojo T. Optimizing solid oxide fuel cell cathode processing route for intermediate temperature operation. Appl. Energy. 2013;104:984–991

[5] J. Alvarado-Flores and L. Ávalos-Rodriguez, "Materiales para ánodos, cátodos y electrolitos utilizados en celdas de combustible de óxido sólido (SOFC)," Rev. Mex. Física, vol. 59, pp. 66–87, 2013.

[6] D. Marinha, L. Dessemond, and E. Djurado, "Electrochemical investigation of oxygen reduction reaction on La 0.6Sr0.4Co0.2Fe0.8O 3-δ cathodes deposited by Electrostatic Spray Deposition," J. Power Sources, vol. 197, pp. 80–87, 2012, doi:10.1016/j.jpowsour.2011.09.049.

[7] R. Jacobs, T. Mayeshiba, J. Booske, and D. Morgan, "Material Discovery and Design Principles for Stable, High Activity Perovskite Cathodes for Solid Oxide Fuel Cells," Adv. Energy Mater., vol. 8, no. 11, 2018, doi: 10.1002/aenm.201702708.

[8] C. Sun, R. Hui, and J. Roller: Cathode materials for solid oxide fuel cells: A review. J Solid State Electrochem. 14, (2010).

[9] Appleby, A.J. and Foulkes, F.R. (1989) Fuel Cell Handbook, Van Nostrand Reinhold, New York.

[10] de Souza, S., Visco, S.J. and de Jonghe, L.C. (1997) 'Thin film solid oxide fuel cell with high performance at low temperature', Solid State Ionics, Vol. 98, Nos. 1–2, pp.57–61.

[11] Minh, N.Q. (1993) 'Ceramic fuel cells', Journal of American Ceramic Society, Vol. 76, No. 3, pp.563–588.

[12] Zhao Y, Xia C, Jia L, Wang Z, Li H, Yu J, Li Y. Recent progress on solid oxide fuel cell: Lowering temperature and utilizing non-hydrogen fuels. Int. J. Hydrogen Energy. 2013; 38:16498–16517.

[13] Bang J. H. and Suslick K. S., "Applications of ultrasound to the synthesis of nanostructured materials," Adv. Mater., vol. 22, no. 10, pp. 1039–1059, 2010, doi: 10.1002/adma.200904093.

[14] R. Abazari et al., "The effect of different parameters under ultrasound irradiation for synthesis of new nanostructured Fe3O4@bio-MOF as an efficient anti-leishmanial in vitro and in vivo conditions," Ultrason. Sonochem., vol. 43, no. December 2017, pp. 248–261, 2018, doi: 10.1016/j.ultsonch.2018.01.022.